Renal Function in Mice with Targeted Disruption of the A Isoform of the Na-K-2Cl Co-Transporter

Mona Oppermann,* Diane Mizel,* Soo Mi Kim,* Limeng Chen,* Robert Faulhaber-Walter,* Yuning Huang,* Cuiling Li,* Chuxia Deng,* Josie Briggs,† Jurgen Schnermann,* and Hayo Castrop*‡

**National Institute of Diabetes and Digestive and Kidney Diseases, National Institutes of Health, Bethesda, and †Howard Hughes Medical Institute, Chevy Chase, Maryland; and ‡Institute of Physiology, University of Regensburg, Regensburg, Germany*

Three different full-length splice isoforms of the Na-K-2Cl co-transporter (NKCC2/BSC1) are expressed along the thick ascending limb of Henle (TAL), designated NKCC2A, NKCC2B, and NKCC2F. NKCC2F is expressed in the medullary, NKCC2B mainly in the cortical, and NKCC2A in medullary and cortical portions of the TAL. NKCC2B and NKCC2A were shown to be coexpressed in the macula densa (MD) segment of the mouse TAL. The functional consequences of the existence of three different isoforms of NKCC2 are unclear. For studying the specific role of NKCC2A in kidney function, NKCC2A−/− mice were generated by homologous recombination. NKCC2A−/− mice were viable and showed no gross abnormalities. Ambient urine osmolarity was reduced significantly in NKCC2A−/− compared with wild-type mice, but water deprivation elevated urine osmolarity to similar levels in both genotypes. Baseline plasma renin concentration and the effects of a high- and a low-salt diet on plasma renin concentration were similar in NKCC2A+/+ and −/− mice. However, suppression of renin secretion by acute intravenous saline loading (5% of body weight), a measure of MD-dependent inhibition of renin secretion, was reduced markedly in NKCC2A−/− mice compared with wild-type mice. Cl and water absorption along microperfused loops of Henle of NKCC2A−/− mice were unchanged at normal flow rates but significantly reduced at supranormal flow. Tubuloglomerular feedback function curve as determined by stop flow pressure measurements was left-shifted in NKCC2A−/− compared with wild-type mice, with maximum responses being significantly diminished. In summary, NKCC2A activity seems to be required for MD salt sensing in the high Cl concentration range. Coexpression of both high- and low-affinity isoforms of NKCC2 may permit transport and Cl-dependent tubuloglomerular feedback regulation to occur over a wider Cl concentration range.

J Am Soc Nephrol 18: 440–448, 2007. doi: 10.1681/ASN.2006091070

The Na-K-2Cl co-transporter (NKCC2), located in the apical membrane of the epithelial cells of the thick ascending limb of Henle (TAL), constitutes the major cellular uptake pathway in this portion of the nephron. In addition, NKCC2 transport activity in macula densa (MD) cells is considered to be the initial step in the signaling chain that links tubular epithelial cells of the TAL with vascular cells of the afferent arteriole (1–5). At least four different full-length splice isoforms of NKCC2 are expressed along the TAL, designated NKCC2A, NKCC2B, NKCC2F, and NKCC2AF (6–10). These isoforms of the transporter are derived from differential splicing of the variable exon 4 of the NKCC2 gene (7,8,11). Exon 4 encodes for amino acids of the second transmembrane domain and the adjacent intracellular loop of NKCC2, a region that has been shown to be involved in the ion-binding characteristics of the co-transporter (11). Cell-specific splicing results in heterogeneous expression of the various NKCC2 isoforms along the TAL. NKCC2F, the most abundant NKCC2 isoform, is expressed in the medullary TAL, NKCC2B mainly in the cortical TAL, and NKCC2A both in medullary and cortical portions of the TAL (6,8,12,13). Isoform-specific *in situ* hybridization indicated that MD cells express only NKCC2B (6), whereas recent functional evidence supports the presence of both NKCC2B and NKCC2A in this part of the nephron (12).

The functional significance of the existence of different isoforms of NKCC2 along the TAL is not entirely clear. Heterologous expression studies have shown marked differences in Cl affinity for the NKCC2 isoforms with a K_m for Cl^- of 9 to 12, 22 to 45, and 110 mM for NKCC2B, NKCC2A, and NKCC2F, respectively (6,10,14). It is conceivable, therefore, that expression of isoforms with different ion affinities allows transport activity in a region where ion concentrations vary over a wide range. The generation of mice with selective deletions of single NKCC2 isoforms seemed to provide an approach to address the functional role of NKCC2 isoforms *in vivo*. We recently reported that mice with inactivation of the B isoform of NKCC2 showed an impairment of Cl absorption along the loop of Henle in the low concentration range that resulted in a right

Received September 30, 2006. Accepted November 20, 2006.

Published online ahead of print. Publication date available at www.jasn.org.

H.C.'s current affiliation is the Institute of Physiology, University of Regensburg, Regensburg, Germany.

Address correspondence to: Dr. Hayo Castrop, NIDDK, NIH, Building 10, Room 4 D51, 10 Center Drive MSC-1370, Bethesda, MD 20892-1370. Phone: 301-435-6579; Fax: 301-435-6587; E-mail: hayo@castrop.com

ISSN: 1046-6673/1802-0440

shift of the tubuloglomerular function curve (12). Thus, the B isoform seems to be especially important for responding to low NaCl concentrations.

In this study, we report that we now have deleted successfully the A isoform of NKCC2, and we summarize our studies in this new mouse model. Like the mice without NKCC2B, NKCC2A−/− mice were viable and were not characterized by a clear salt-losing phenotype. Short-term MD-dependent suppression of renin secretion was blunted in NKCC2A−/− mice. Maximum tubuloglomerular feedback (TGF) responses were reduced in NKCC2A−/− mice. Together with our data from NKCC2B−/− mice, we suggest that the low Cl–affinity NKCC2A and the high Cl–affinity NKCC2B along the TAL and in the MD may cooperate to facilitate efficient salt absorption over a wider range of Cl concentrations than is achievable by each isoform alone.

Materials and Methods

Generation of NKCC2A−/− Mice

All animal studies were examined and approved by the Animal Use and Care Committee of the National Institute of Diabetes and Digestive and Kidney Diseases and by the Animal Care Committee of the University of Regensburg. NKCC2A−/− mice were generated according to the strategy described previously for NKCC2B−/− mice (12). A targeting vector was generated to introduce premature stop codons into exon 4A of the NKCC2 gene (Figure 1). Homologous arms were generated by long-distance PCR (Roche, Indianapolis, IN). Primers used were 5′-GGAAGGTTATTTGGGCTTGGTCCTG-3′ and 5′-ACACCGAGACCTCAGTTGAGAGG-3′ for the upstream arm and 5′-GATTATCATCGGCTTAGCCGTGACAG-3′ and 5′-GGAGTTGCCACACTACATGGGCTC-3′ for the downstream arm. 129SvEv ES cells were electroporated with the NotI-linearized targeting vector. Primers that were used for PCR screening of the clones were 5′-CGCAGCGCATCGCCTTCTATCGCCTTC-3′ and 5′-CCACGGTGATGGAACCGATGATG-3′. For excision of the loxP-flanked neo cassette, homozygous NKCC2A−/− mice were crossed with EIIa-Cre mice (15). Progeny that lacked the neo gene was intercrossed to obtain homozygous NKCC2A−/− mice and wild-type littermates.

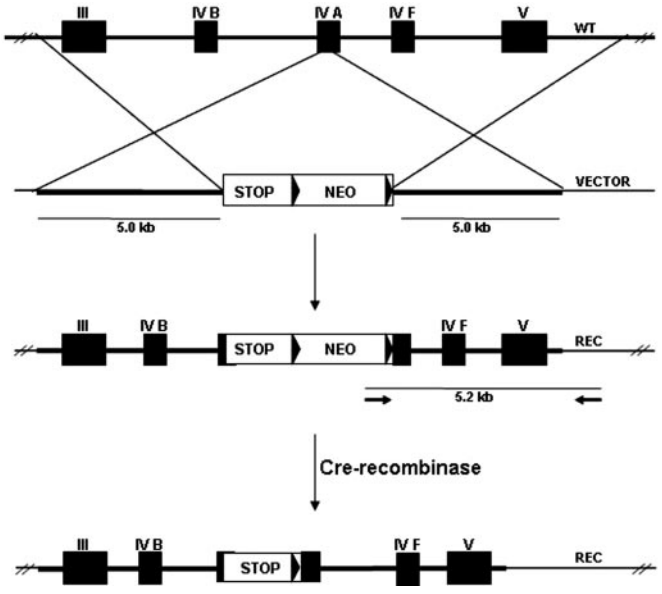

Figure 1. Targeting strategy showing introduction of premature stop codons into exon 4A of the NKCC2 gene (*Slc12a1*); the vector also contained the FLAG peptide coding sequence upstream of the stop codons (not shown in the scheme). Arrows indicate PCR-based screening strategy for alleles that had undergone homologous recombination. The neomycin resistance cassette flanked by loxP sites was removed by crossing with EIIa-Cre mice.

Analysis of the Mutated Transcripts of NKCC2A−/− Mice

NKCC2A mutated transcripts as well as the remaining NKCC2B and NKCC2F isoforms were analyzed by reverse transcriptase–PCR (RT-PCR) and sequencing (12).

Localization of NKCC2B, NKCC2A, and NKCC2F Transcripts in Kidney Regions

The localization of the three different isoforms of NKCC2 was determined by real-time RT-PCR on RNA derived from cortex and outer and inner medulla (12).

NKCC2 Immunoblotting

Western blotting was performed according to standard protocols using a polyclonal anti-NKCC2 antibody (gift from Dr. M. Knepper, NIH, Bethesda, MD). Coomassie blue–stained gels served as loading controls.

BP and Heart Rate

BP and heart rate were determined by radiotelemetry in NKCC2A+/+ and −/− mice ($n = 5$ each) (16). Data were collected every hour, and results are given as averages of four successive dark (6 p.m. to 6 a.m.) and light (6 a.m. to 6 p.m.) cycles.

Plasma Chemistry and Plasma Volume

Plasma chemistry was determined by standard methods in plasma that was collected from the vena cava of freshly anesthetized mice. Plasma volume of conscious mice was measured as the distribution volume of injected Evans Blue (17). During a short isoflurane anesthesia, 30 μl of a 5-mg/ml Evans blue solution was injected retro-orbitally, and blood collections of approximately 5 μl were made by tail-vein puncture at 7 and 15 min. Absorbance at 620 nm was measured in a 1:5 dilution of plasma in a ND-1000 Nanodrop spectrophotometer and compared with a standard curve.

Urine Osmolarity

Urine osmolarities under ambient conditions and after 48 h of water restriction were determined in spot urine samples that were obtained by transurethral catheterization of female mice.

Blood Collection and Plasma Renin Determination

Blood was collected from conscious mice by puncture of the submandibular vessels with a 19-G needle and collection of approximately 20 μl of the emerging blood into an EDTA-containing microhematocrit tube. Plasma renin concentration (PRC) was measured with a RIA kit (DiaSorin, Stillwater, MN), as described previously (18). In 36 female mice of various genotypes, we compared PRC measurements in blood taken by tail-vein puncture followed by mandibular bleeding 2 wk later. PRC was consistently lower in mandibular blood (847 ± 70 ng angiotensin I (AngI)/ml per hr) than in tail-vein blood (2067 ± 106 ng AngI/ml per hr). We ascribe this difference to the much shorter and less stressful intervention in the case of mandibular collections.

For assessment of renin secretion after inhibition of MD salt transport, a single dose of furosemide (40 mg/kg) was injected intraperito-

neally, and blood samples were drawn 60 min later. MD-dependent inhibition of renin release was determined in short-term and long-term experiments. In short-term experiments, mice received a single intravenous (tail vein) injection of saline (5% of body weight) and blood samples were collected 60 min later (12,16,19). For chronic modulation of the renin-angiotensin system, mice were subjected to the following treatments: (*1*) Control group: Mice were fed a standard rodent diet (0.3% NaCl [wt/wt]) for 1 wk; (*2*) salt-deficient group: After injection of a single dose of furosemide (40 mg/kg intraperitoneally), mice received a salt-deficient diet (0.03% NaCl [wt/wt]) for 1 wk; (*3*) salt load group: Mice were fed a high-salt diet (4% NaCl [wt/wt]) for 1 wk.

GFR

GFR of conscious mice was measured by FITC inulin clearance after a single retro-orbital injection and consecutive blood sampling from the tail vein (20). The method was modified in our laboratory to reduce the required blood withdrawal as described in detail recently (21).

Micropuncture Experiments

Measurements of stop flow pressure (P_{SF}) during perfusion of loop of Henle were done as described previously (5,12). When P_{SF} had stabilized, perfusion rate of loop of Henle was increased to 30 nl/min and maximum P_{SF} responses were determined. Perfusion rates then were decreased to 20, 15, 10, 7.5, 5, and 0 nl/min and maintained until steady states were achieved at each flow rate. The perfusion fluid contained (in mM/L) 136 NaCl, 4 $NaHCO_3$, 4 KCl, 2 $CaCl_2$, and 7.5 urea and 100 mg/100 ml FD&C green (Keystone, Bellefonte, PA). Using the same perfusion approach and perfusion fluid, Cl reabsorption along superficial loops of Henle was determined at flow rates of 6 and 15 nl/min as described previously (12).

Statistical Analyses

Unpaired *t* test was used to compare two values between different animals. Multiple groups were analyzed with ANOVA followed by Bonferroni post test. $P < 0.05$ was considered significant.

Table 1. Average concentrations of a number of plasma constituents in NKCC2A+/+ ($n = 8$) and NKCC2A−/− mice ($n = 10$)[a]

Parameter	NKCC2A+/+		NKCC2A−/−	
	Mean	SEM	Mean	SEM
Glucose (mg/dl)	235	13.78	221	6.42
Cholesterol (mg/dl)	79	4.94	66	7.60
Triglycerides (mg/dl)	41	3.78	33	5.21
Na (mmol/L)	148	0.46	149	0.75
K (mmol/L)	3.4	0.08	3.4	0.17
Cl (mmol/L)	117	0.70	118	0.67
Ca (mmol/L)	2.15	0.03	2.13	0.02
Mg (mmol/L)	0.90	0.02	0.81[b]	0.03
P (mg/dl)	5.7	0.29	5.8	0.24
Creatinine (mg/dl)	0.3	0.00	0.3	0.02
BUN (mg/dl)	23	1.11	20	1.39
Alkaline phosphatase (U/L)	70	5.09	65	6.40
ALT/GPT (U/L)	20	1.53	19	1.20
AST/GOT (U/L)	43	1.21	45	3.03
LDH (U/L)	114	16.10	92	8.87
Amylase (U/L)	1063	53.37	1048	70.10
Uric acid (mg/dl)	0.7	0.05	0.7	0.10
Total protein (g/dl)	4.3	0.09	4.1	0.14
Albumin (g/dl)	2.7	0.10	2.7	0.04

[a]ALT/GPT, alanine aminotransferase/glutamate pyruvate transaminase; AST/GOT, aspartate aminotransferase/glutamate oxaloacetic transaminase; BUN, blood urea nitrogen; LDH, lactate dehydrogenase.
[b]$P < 0.05$.

Results

Targeting of NKCC2A

NKCC2A−/− mice were viable and showed no obvious anatomic or behavioral abnormalities. Furthermore, both male and female NKCC2A−/− mice were fertile. Wild-type, heterozygous, and homozygous genotypes in offspring of heterozygous crosses were obtained in near Mendelian ratio of 22.8, 48.2, and 29.0% for NKCC2A+/+, +/−, and −/−, respectively. As can be seen in Table 1, measurement of a panel of plasma constituents revealed no significant differences between wild-type and NKCC2A−/− mice with the exception of reduced plasma Mg^+ concentrations in NKCC2A−/− mice (0.9 ± 0.02 and 0.81 ± 0.03 mmol/L for NKCC2A+/+ and −/−, respectively; $n = 8$ and 10; $P = 0.019$). Plasma volume was similar in both genotypes (4.6 ± 0.5 *versus* 4.7 ± 0.6% of body weight; $P = 0.27$).

Analysis of NKCC2 transcripts after removal of the neomycin cassette revealed that NKCC2B and NKCC2F mRNA were not influenced by the modification of exon 4A. However, two different transcripts were found for the mutated NKCC2A (Figure 2). In one of these, correct splicing was preserved fully, whereas in the other, exon 4A was flanked by additional intronic sequences followed by exon 4F sequence. Both transcripts possess multiple stop codons in all reading frames, ensuring premature termination of translation specifically of NKCC2A. To assess whether NKCC2A deletion influences the quantity and the localization of the remaining isoforms, we determined mRNA levels of NKCCB and NKCC2F. Expression of the dominant F isoform of NKCC2 was identical in NKCC2A−/− and wild-type mice, with highest expression levels in the inner stripe of the outer medulla. NKCC2B mRNA was found in both cortex and outer medulla, mainly in the outer stripe. In contrast to NKCC2F, NKCC2B mRNA expression was upregulated substantially in NKCC2A−/− mice compared with NKCC2A+/+ mice (Figure 3). NKCC2A mRNA in wild-type mice was present in both cortex and medulla. In view of the upregulation of NKCC2B mRNA expression, we determined total NKCC2 protein abundance. Total NKCC2 protein levels as determined by immunoblotting were slightly reduced in NKCC2A−/− mice (−26%; $P = 0.11$; Figure 4).

Urine Osmolarity, Concentrating Ability, and GFR

Ambient urine osmolarity (Figure 5) averaged 1466 ± 81 mosmol/L in NKCC2A−/− mice ($n = 26$) and 1847 ± 133 mosmol/L in NKCC2A+/+ mice ($n = 21$; $P = 0.014$). Water restriction for 48 h caused urine osmolarity to increase to a

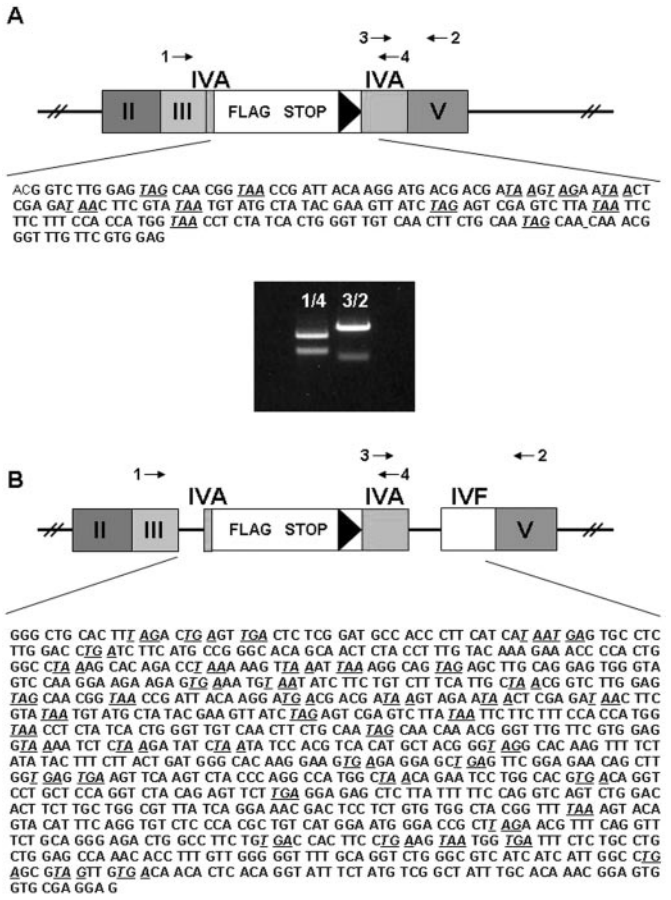

Figure 2. Sequencing of NKCC2A transcripts after removal of the neomycin resistance cassette. Two different mutated transcripts were identified. (A) Correct splicing was preserved. (B) Additional intronic sequences were present up- and downstream of exon 4A as well as the full sequence of exon 4F. Both targeting events led to the introduction of several premature stop codons in all reading frames (underlined italic base triplets). Inset shows reverse transcriptase–PCR products that were generated using primers as indicated in A. Short PCR products correspond to correctly spliced mutated transcripts (shown in A), whereas long PCR products correspond to transcripts shown in B.

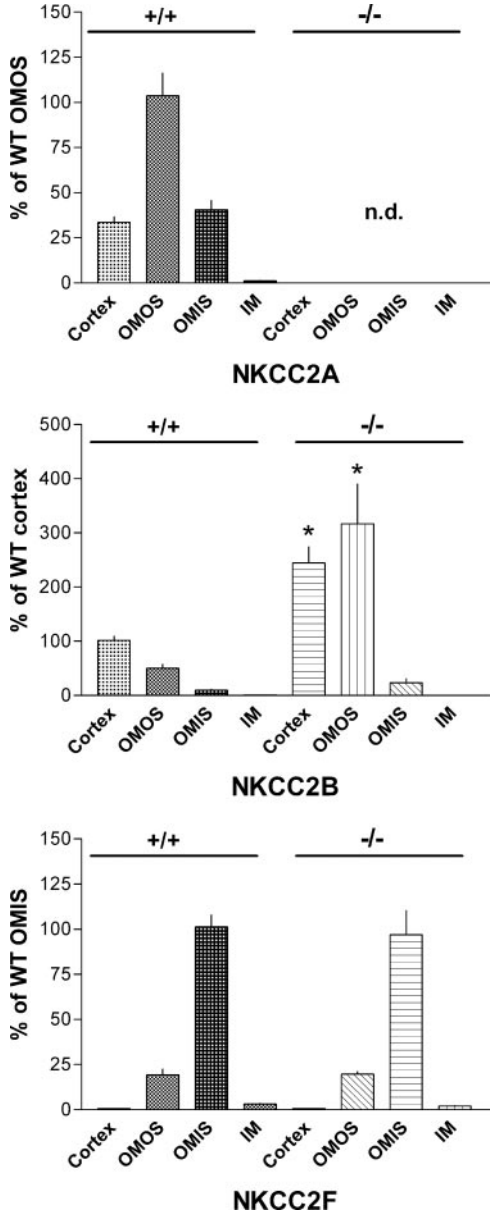

Figure 3. Expression of NKCC2A, NKCC2B, and NKCC2F mRNA in kidney regions of NKCC2A+/+ and −/− mice. Real-time PCR was performed using isoform-specific TaqMan probes and β-actin as a reference; data are given as percentage of the zone with highest expression levels of the respective isoform ($n = 6$ each). IM, inner medulla; OMIS, outer medulla inner stripe; OMOS, outer medulla outer stripe; n.d., not detected (a probe specific for the wild-type NKCC2A transcript was used).

comparable extent in both groups of mice, to 3979 ± 157 in wild-type ($n = 9$) and to 3802 ± 186 mosmol/L in NKCC2A−/− mice ($n = 11$; $P = 0.49$). GFR did not differ between wild-type and NKCC2A−/− mice, averaging 1375 ± 259 *versus* 1172 ± 246 μl/min per 100 g body wt ($P = 0.18$).

BP and Heart Rate

BP and heart rate, measured by telemetry in five wild-type and five NKCC2A−/− mice, did not differ significantly between genotypes (Figure 6). Systolic and diastolic arterial pressures during the active night period averaged 133 ± 7 and 103 ± 5 mmHg in wild-type mice and 128 ± 6 and 97 ± 5 mmHg in NKCC2A−/− mice ($P = 0.58$ and 0.69, respectively). During the inactive light period, systolic and diastolic pressures were 122 ± 5 and 92 ± 5 mmHg in wild-type mice and 115.5 ± 6 and 86 ± 5 mmHg in NKCC2A−/− mice ($P = 0.49$ and 0.95, respectively). The circadian variations in BP did not differ between genotypes.

Plasma Renin and Plasma Aldosterone Concentrations

Baseline PRC in mice that were on a standard rodent diet was similar in NKCC2A+/+ ($n = 23$) and NKCC2A−/− mice ($n = 30$), averaging 664 ± 70 and 618 ± 65 ng AngI/ml per h, respectively ($P = 0.64$). As shown in Figure 7, acute administration of the loop diuretic furosemide, an intervention that is

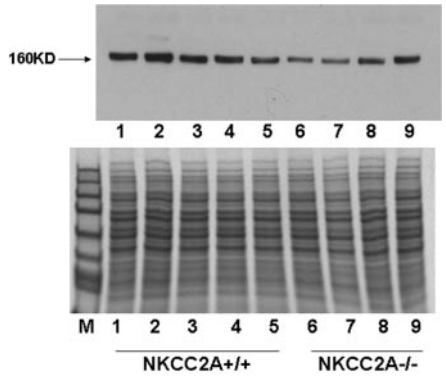

Figure 4. Quantification of NKCC2 by immunoblotting (top) and Coomassie blue staining for total protein as loading control.

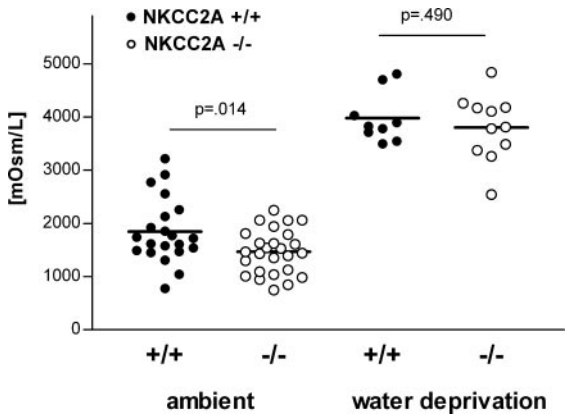

Figure 5. Osmolarity of spot urine samples that were collected by urethral catheterization of female NKCC2A+/+ and −/− mice before and after water deprivation.

thought to activate maximally the MD pathway of renin control, increased PRC to 2923 ± 409 ng AngI/ml per h in NKCC2A−/− mice (n = 9; P = 0.0001 *versus* baseline) and to 3439 ± 535 ng AngI/ml per h in NKCC2A+/+ mice (n = 9; P = 0.0006 *versus* baseline, P = 0.46 between genotypes). In mice that were kept on a low-salt diet for 1 wk, PRC increased from 544 ± 88 to 1126 ± 136 in NKCC2+/+ (n = 10; P = 0.010 *versus* basal) and from 700 ± 149 to 1652 ± 299 ng AngI/ml per h in NKCC2A−/− mice (n = 10; P = 0.012 *versus* basal, P = 0.13 between genotypes). Exposure to a high-salt diet for 1 wk reduced PRC to approximately the same extent in both genotypes, averaging 213 ± 59 in wild-type mice (n = 10; P = 0.003 *versus* basal) and 227 ± 44 ng AngI/ml per h in NKCC2A−/− (n = 10; P = 0.004 *versus* basal, P = 0.85 between genotypes; Figure 8).

The acute and rapid administration of isotonic saline has been used as a measure to increase luminal NaCl concentration at the MD and therefore to test the inhibitory component of MD-dependent control of renin secretion (3,16,22). In agreement with earlier observations, wild-type mice (n = 13) that received a single intravenous injection of saline (5% of body weight) responded with a consistent suppression of PRC from 673 ± 115 to 389 ± 54 ng AngI/ml per h (P = 0.006), a relative decrease of 42% (Figure 9). In contrast, the PRC response to saline in NKCC2A−/− mice (n = 17) consisted of a nonsignificant 16% decrease from 509 ± 64 to 429 ± 62 ng AngI/ml per h (P = 0.14; Figure 9). To assess the impact of a nonspecific effect of volume expansion, we compared the effect of NaCl with that of $NaHCO_3$ given in an equivalent amount. $NaHCO_3$ injections had no significant effect on PRC in either genotype (data not shown). As shown in Table 2, plasma aldosterone concentrations did not differ between wild-type and NKCC2A−/− mice.

Distal Tubular Cl Concentration

Loop of Henle Cl and fluid reabsorption was assessed by measurement of Cl concentrations and fluid flow rates in distal tubular fluid samples of superficial nephrons that were microperfused *in situ* at two different flow rates (Figure 10). At a tubular perfusion rate of 6 nl/min, distal Cl concentrations were not significantly different between wild-type and NKCC2A−/− mice, averaging 64.6 ± 6.2 and 73.6 ± 3.3 mmol/L (n = 11 and 12; P = 0.20). At a tubular perfusion of 15 nl/min, however, distal Cl concentrations in NKCC2A−/− exceeded those in NKCC2A+/+ by 15.7 mmol/L, averaging 98.2 ± 3.6 *versus* 82.5 ± 4.0 mmol/L in NKCC2A−/− (n = 15) and wild type mice (n = 11), respectively (P = 0.008; Figure 10A). Absolute Cl absorption was similar in wild-type and NKCC2A−/− mice at low perfusion (662 ± 31 *versus* 671 ± 16 pmol/min; P = 0.79) but was significantly lower in NKCC2A−/− compared with NKCC2A+/+ at high perfusion flows (1167 ± 58 *versus* 1436 ± 53 pmol/min; P = 0.003; Figure 10B). Similarly, water absorption was lower in loops of NKCC2A−/− at high flow (5.5 ± 0.5 *versus* 7.0 ± 0.4 nl/min; P = 0.031) but similar at low flow rates (3.7 ± 0.3 *versus* 3.3 ± 0.3 nl/min in wild-type mice; P = 0.36). Thus, fractional Cl absorption at high perfusion rates also was reduced in NKCC2A−/− compared with NKCC2A+/+ (36.7 ± 3.0 *versus* 46.5 ± 2.7%; P = 0.003).

TGF

TGF responses were determined by measurement of proximal tubular P_{SF} during loop perfusion rates of 0, 5, 7.5, 10, 15, 20, and 30 nl/min. TGF responses were investigated in nephrons of eight male wild-type and five male NKCC2A−/− mice (n = 11 nephrons each). At zero perfusion, P_{SF} was similar in nephrons from NKCC2A+/+ and −/− mice (45.3 ± 2.2 *versus* 45.8 ± 2.2 mmHg; P = 0.89). P_{SF} at increasing perfusion rates of 5, 7.5, 10, 15, 20, and 30 nl/min decreased to 99.7 ± 1.1, 97.7 ± 1.3, 91.3 ± 2.2, 81.6 ± 3.7, 78.9 ± 3.0, and 76.1 ± 2.9% of P_{SF} at zero perfusion in nephrons from wild-type mice compared with 95.2 ± 1.0, 90.8 ± 1.6, 87.8 ± 1.9, 84.9 ± 2.8, 84.8 ± 2.5, and 84.7 ± 2.0% in nephrons from NKCC2A−/− mice (P = 0.007, 0.004, 0.251, 0.483, 0.137, and 0.021, respectively). Thus, TGF responsiveness was augmented in NKCC2A−/− mice at low perfusion rates (5 and 7.5 nl/min), whereas maximum responses at the saturating perfusion rate of 30 nl/min were reduced in NKCC2A−/− compared with wild-type mice (Figure 11).

Discussion

These studies are a continuation of our attempts to evaluate the functional significance of the presence of various NKCC2

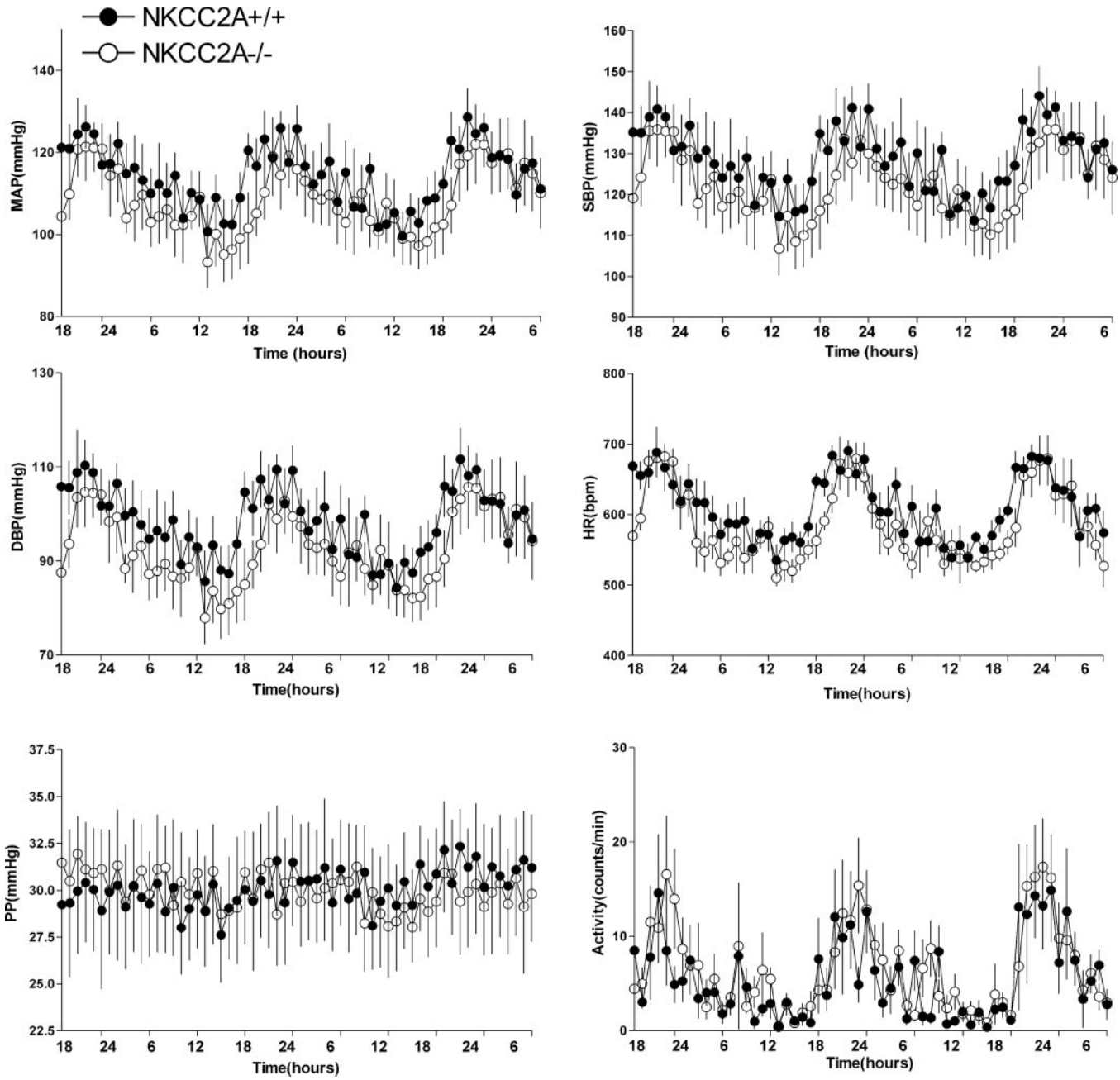

Figure 6. Mean arterial pressure (MAP), systolic BP (SBP), diastolic BP (DBP), pulse pressure (PP), heart rate (HR), and activity scores for five wild-type and five NKCC2A−/− mice recorded over a period of 60 h (one measurement each hour).

isoforms along the TAL. We showed previously that introduction of premature stop codons by homologous recombination was successful in generating mice with a specific deficiency of the B isoform of NKCC2 without interfering with normal splicing of the other isoforms (12). Using a similar approach, we now have succeeded in creating a mouse model with specific inactivation of the A isoform of NKCC2. NKCC2A normally is expressed in both medullary and cortical portions of the TAL, and it also is found in MD cells (12,13).

Our study shows that introduction of stop codons into exon 4A, specific for the A isoform of the co-transporter, led to premature termination of translation of the A isoform only, without compromising the expression of the remaining isoforms NKCC2B and NKCC2F. However, in contrast to the previously described inactivation of NKCC2B, analysis of the mutated NKCC2A transcripts revealed that besides the predicted mutated transcript, an additional mis-spliced NKCC2A mRNA that integrates intronic sequences up- and downstream of exon 4A exists. Although the exact reason for this abnormality remains unclear, this finding highlights the sensitivity of the splicing machinery to minor changes in sequence and length of a specific exon (23,24). Nevertheless, the presence of stop codons guarantees premature stop of translation of this abnormal NKCC2A transcript. From our sequence analysis, we as-

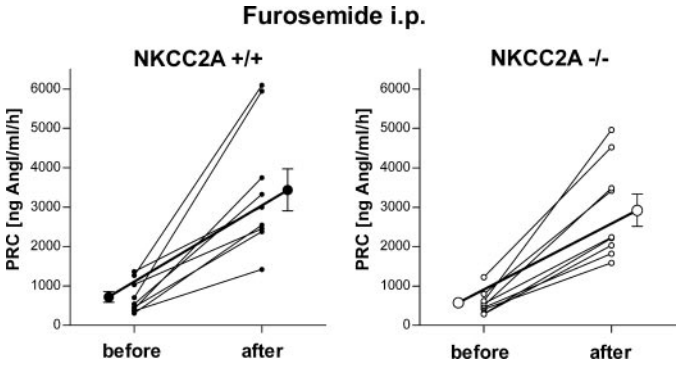

Figure 7. Plasma renin concentration (PRC) before and 60 min after acute administration of furosemide (40 mg/kg intraperitoneally) in NKCC2A+/+ (left) and −/− mice (right); lines connect data from the same mice.

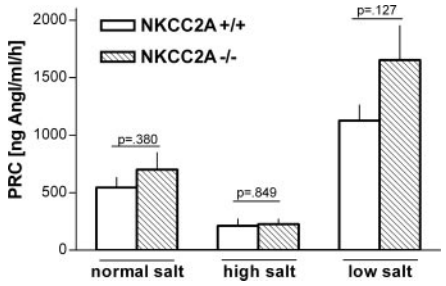

Figure 8. PRC in NKCC2A+/+ and NKCC2A−/− mice that were fed a standard rodent diet (0.3% NaCl), high-salt diet (4% NaCl), or low-salt diet (0.03% NaCl after a single dose of 40 mg/kg furosemide). PRC was determined after 1 wk of the respective treatment; $n = 10$ for each group.

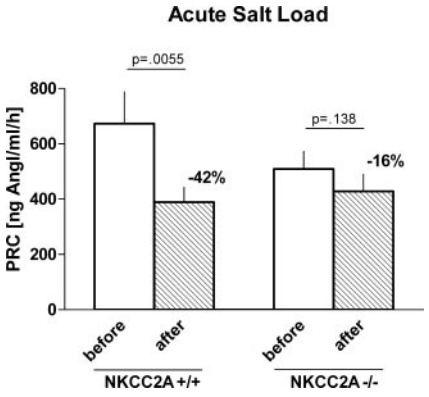

Figure 9. Effect of an intravenous administration of saline (5% of body weight) on PRC in NKCC2A+/+ ($n = 13$) and −/− mice ($n = 17$). Blood samples were taken 60 min after the injection; percentages indicate relative decrements of PRC.

Table 2. Plasma aldosterone concentrations (pg/ml) in NKCC2A+/+ and −/− mice after 1 wk on control (0.3% NaCl), high-salt (4% NaCl), or low-salt diet (0.03% NaCl after a single dose of 40 mg/kg furosemide intraperitoneally)[a]

Aldosterone (pg/ml)	Normal Salt	High Salt	Low Salt
NKCC2A+/+	264 ± 52	56 ± 21	672 ± 108
NKCC2A−/−	385 ± 39	38 ± 15	700 ± 58

[a]Data are means ± SEM; $n = 10$ for each group.

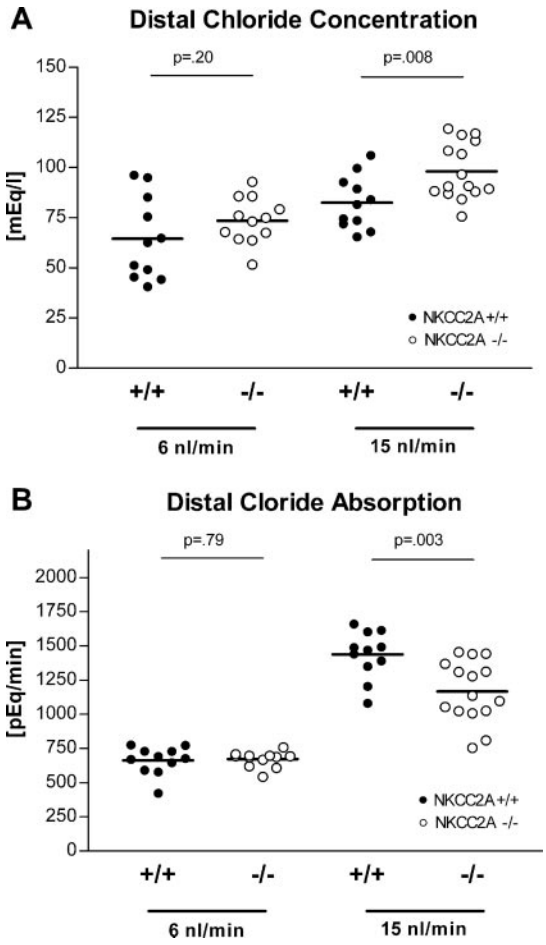

Figure 10. (A) Cl concentration in individual samples of distal tubular fluid of microperfused superficial loops of Henle in NKCC2A+/+ (●) and NKCC2A−/− mice (○); data are shown for perfusion rates of 6 and 15 nl/min. (B) Absolute Cl absorption along the loop of Henle perfused at 6 and 15 nl/min. *$P < 0.05$.

sume that the mis-spliced mutant NKCC2A transcript may be related to the known NKCC2AF tandem transcript (7,13). However, because the mutated exon 4A is located upstream of exon 4F, a possible NKCC2AF transcript would be predicted also to be nonfunctional. In our previous study in mice with NKCC2B deletion, we found that the expression of NKCC2A and NKCC2F remained unaltered (12). In contrast, mutation of NKCC2A led to an increased expression of NKCC2B in both cortex and outer stripe of the outer medulla, the primary sites of NKCC2A expression. However, the upregulation of NKCC2B expression could not compensate fully for the loss of NKCC2A protein as judged from NKCC2 protein determination by Western blotting.

Inactivation of the entire NKCC2 gene is characterized by a severe salt-losing phenotype and by the death of most animals

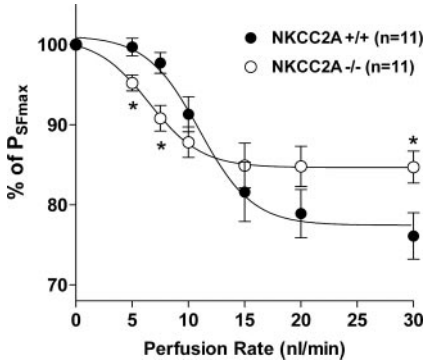

Figure 11. Change of stop flow pressure (P_{SF}) expressed as percentage reduction of P_{SFmax} (P_{SF} at zero loop flow) in response to stepwise increases of loop of Henle flow rates in wild-type (●) and NKCC2A−/− mice (○). Curve fitting was done by nonlinear regression analysis using GraphPad Prism.

within the first 2 wk of postnatal life (25). After specific inactivation of NKCC2A, however, survival was not affected and there were no overt symptoms of volume depletion or obvious renal structural changes. In this regard, NKCC2A−/− mice resemble NKCC2B−/− mice, which also display an inconspicuous phenotype (12). The absence of clear symptoms of salt deficiency with single isoform deletions along the cortical TAL is congruent with functional overlaps or compensatory adjustments between the A and B isoforms of the co-transporter. Nevertheless, NaCl and fluid reabsorption along the TAL of NKCC2A−/− mice clearly was reduced during perfusion with supranormal flow rates. Therefore, NKCC2A may be required for the prevention of a salt-absorption deficit under conditions of elevated rates of NaCl delivery to the cortical TAL, where NKCC2B-driven transport has reached saturation. This notion is consistent with our recent findings in NKCC2B−/− mice in which absolute and fractional loop Cl absorption were reduced at low but not at high perfusion flow rates (12).

A functional NKCC2 activity has been shown to be required for the translation of changes in luminal NaCl concentration into changes of vascular tone and renin secretion. In keeping with our interest in the function of the juxtaglomerular apparatus, we have made an attempt to identify the specific roles of NKCC2A and NKCC2B in TGF and MD-dependent renin secretion. In contrast to earlier evidence, recent isoform-specific *in situ* hybridization in the mouse clearly showed coexpression of both NKCC2B and NKCC2A mRNA in MD cells (12), a finding that is consistent with the conclusion from RT-PCR studies in the rat (13). Our results show that maximum TGF responses are reduced to approximately half normal in NKCC2A−/− mice compared with wild-type mice, indicating that MD sensor function becomes dependent on NKCC2A-mediated transport activity when tubular salt concentrations are above normal levels. We suggest that changes in Cl concentration above approximately 30 mM are not detected because the B isoform has a Cl affinity of approximately 10 mM and therefore should operate at close to full saturation in the high concentration range. Our observation that TGF responsiveness was enhanced in NKCC2A−/− mice compared with wild-type mice at concentrations below normal may be the result of the increased expression of NKCC2B in NKCC2A−/− mice. In addition, it might indicate that Cl concentrations at the MD at a given subnormal perfusion rate are higher in NKCC2A−/− compared with NKCC2A+/+ as a result of loss of NKCC2A in upstream portions of the TAL. To some extent, these studies are complementary to observations in NKCC2B−/− mice in which TGF function curves were right-shifted, suggesting that NKCC2B is required to maintain a normal TGF responsiveness to subnormal flow. Overall, our data suggest a successive engagement of NKCC2B and NKCC2A because NaCl concentrations at the MD are altered over the TGF-relevant Cl concentration range between 0 and 60 mM (26), Cl concentrations at which changes of NKCC2 transport activity would be expected on the basis of a K_m of approximately 9 to 12 mM for NKCC2B and 22 to 45 mM for NKCC2A (6,10,14).

Whereas basal PRC was not significantly different between NKCC2A−/− and wild-type mice, the acute suppression of PRC in response to acute salt loading by intravenous injection of saline (19,22) was attenuated greatly in NKCC2A−/− mice. Infusion of a similar amount of saline to rats was shown to increase distal tubular Cl concentration by approximately 50%, and this was associated with a suppression of renin secretion by roughly 50% (19). Absence of the renin-inhibitory response in NKCC2A−/− mice is consistent with the notion that NKCC2A-dependent Cl transport activity initiates MD-dependent signaling in the high NaCl concentration range. Previous observations in NKCC2B−/− mice showed that acute salt loading enhanced the suppression of PRC that was seen in wild-type mice (12). As a result of loss of NKCC2B activity in portions of the TAL upstream of the MD segment, Cl concentrations during salt exposure may have exceeded those in wild-type mice, leading to enhanced suppression of renin secretion that was mediated by intact NKCC2A transport activity (12). In contrast to acute salt loading, chronic exposure to a high-salt diet led to a suppression of PRC that was not modified significantly by the presence or absence of NKCC2A. Therefore, the contribution of the MD in the long-term control of renin secretion might be minor or fully compensated by other mechanisms. It is noteworthy that a similar divergence between the effects of acute and chronic salt loading has been observed in adenosine 1A receptor–deficient mice. Whereas the changes of PRC by salt diets largely were normal, the suppression of PRC in response to acute salt loading as well as the decrease in renin secretion that was caused by an increased renal perfusion pressure in the isolated perfused kidney were abolished in adenosine 1A receptor–deficient mice (16,27,28).

Conclusion

We generated mice with specific deletion of the A isoform of NKCC2. NKCC2A−/− mice are viable and show no gross abnormalities and no severe salt-losing phenotype. However, NKCC2A activity seems to be involved crucially in MD salt sensing in the high concentration range. Our data suggest that coexpression of the low Cl–affinity NKCC2A and the high Cl–affinity NKCC2B in the MD segment permits efficient salt sensing over a wide range of salt concentrations.

Acknowledgments

This work was supported by intramural funds from the National Institute of Diabetes and Digestive and Kidney Diseases. M. Oppermann is the recipient of a Visiting Fellowship of the National Institute of Diabetes and Digestive and Kidney Diseases. H. Castrop was supported by a grant from the Deutsche Forschungsgemeinschaft (SFB699/A4).

Disclosures

None.

References

1. Bell PD, Lapointe JY: Characteristics of membrane transport processes of macula densa cells. *Clin Exp Pharmacol Physiol* 24: 541–547, 1997
2. Bell PD, Lapointe JY, Cardinal J, Chang YS: Transport pathways in macula densa cells. *Kidney Int Suppl* 32: S59–S64, 1991
3. Lapointe JY, Bell PD, Cardinal J: Direct evidence for apical Na+:2Cl−:K+ cotransport in macula densa cells. *Am J Physiol* 258: F1466–F1469, 1990
4. Obermuller N, Kunchaparty S, Ellison DH, Bachmann S: Expression of the Na-K-2Cl cotransporter by macula densa and thick ascending limb cells of rat and rabbit nephron. *J Clin Invest* 98: 635–640, 1996
5. Wright FS, Schnermann J: Interference with feedback control of glomerular filtration rate by furosemide, triflocin, and cyanide. *J Clin Invest* 53: 1695–1708, 1974
6. Gimenez I, Isenring P, Forbush B: Spatially distributed alternative splice variants of the renal Na-K-Cl cotransporter exhibit dramatically different affinities for the transported ions. *J Biol Chem* 277: 8767–8770, 2002
7. Igarashi P, Vanden Heuvel GB, Payne JA, Forbush, B 3rd: Cloning, embryonic expression, and alternative splicing of a murine kidney-specific Na-K-Cl cotransporter. *Am J Physiol* 269: F405–F418, 1995
8. Payne JA, Forbush B 3rd: Alternatively spliced isoforms of the putative renal Na-K-Cl cotransporter are differentially distributed within the rabbit kidney. *Proc Natl Acad Sci U S A* 91: 4544–4548, 1994
9. Plata C, Meade P, Hall A, Welch RC, Vazquez N, Hebert SC, Gamba G: Alternatively spliced isoform of apical Na(+)-K(+)-Cl(−) cotransporter gene encodes a furosemide-sensitive Na(+)-Cl(−) cotransporter. *Am J Physiol Renal Physiol* 280: F574–F582, 2001
10. Plata C, Meade P, Vazquez N, Hebert SC, Gamba G: Functional properties of the apical Na+-K+-2Cl− cotransporter isoforms. *J Biol Chem* 277: 11004–11012, 2002
11. Gagnon E, Bergeron MJ, Brunet GM, Daigle ND, Simard CF, Isenring P: Molecular mechanisms of Cl- transport by the renal Na(+)-K(+)-Cl− cotransporter. Identification of an intracellular locus that may form part of a high affinity Cl(−)-binding site. *J Biol Chem* 279: 5648–5654, 2004
12. Oppermann M, Mizel D, Huang G, Li C, Deng C, Theilig F, Bachmann S, Briggs J, Schnermann J, Castrop H: Macula densa control of renin secretion and preglomerular resistance in mice with selective deletion of the B isoform of the Na,K,2Cl Co-transporter. *J Am Soc Nephrol* 17: 2143–2152, 2006
13. Yang T, Huang YG, Singh I, Schnermann J, Briggs JP: Localization of bumetanide- and thiazide-sensitive Na-K-Cl cotransporters along the rat nephron. *Am J Physiol* 271: F931–F939, 1996
14. Gagnon E, Forbush B, Caron L, Isenring P: Functional comparison of renal Na-K-Cl cotransporters between distant species. *Am J Physiol Cell Physiol* 284: C365–C370, 2003
15. Xu X, Li C, Garrett-Beal L, Larson D, Wynshaw-Boris A, Deng CX: Direct removal in the mouse of a floxed neo gene from a three-loxP conditional knockout allele by two novel approaches. *Genesis* 30: 1–6, 2001
16. Kim SM, Mizel D, Huang YG, Briggs JP, Schnermann J: Adenosine as a mediator of macula densa-dependent inhibition of renin secretion. *Am J Physiol Renal Physiol* 290: F1016–F1023, 2006
17. Zhang H, Zhang A, Kohan DE, Nelson RD, Gonzalez FJ, Yang T: Collecting duct-specific deletion of peroxisome proliferator-activated receptor gamma blocks thiazolidinedione-induced fluid retention. *Proc Natl Acad Sci U S A* 102: 9406–9411, 2005
18. Castrop H, Huang Y, Hashimoto S, Mizel D, Hansen P, Theilig F, Bachmann S, Deng C, Briggs J, Schnermann J: Impairment of tubuloglomerular feedback regulation of GFR in ecto-5′-nucleotidase/CD73-deficient mice. *J Clin Invest* 114: 634–642, 2004
19. Lorenz JN, Kotchen TA, Ott CE: Effect of Na and Cl infusion on loop function and plasma renin activity in rats. *Am J Physiol* 258: F1328–F1335, 1990
20. Qi Z, Whitt I, Mehta A, Jin J, Zhao M, Harris RC, Fogo AB, Breyer MD: Serial determination of glomerular filtration rate in conscious mice using FITC-inulin clearance. *Am J Physiol Renal Physiol* 286: F590–F596, 2004
21. Chen L, Kim SM, Oppermann M, Faulhaber-Walter R, Huang YG, Mizel D, Chen M, Sequeira Lopez ML, Weinstein LS, Gomez RA, Briggs JP, Schnermann JB: Regulation of renin in mice with cre recombinase-mediated deletion of G protein Gsalpha in juxtaglomerular cells. *Am J Physiol Renal Physiol* July 5, 2006 [epub ahead of print]
22. Kirchner KA, Kotchen TA, Galla JH, Luke RG: Importance of chloride for acute inhibition of renin by sodium chloride. *Am J Physiol* 235: F444–F450, 1978
23. Sterner DA, Carlo T, Berget SM: Architectural limits on split genes. *Proc Natl Acad Sci U S A* 93: 15081–15085, 1996
24. Xie J, Black DL: A CaMK IV responsive RNA element mediates depolarization-induced alternative splicing of ion channels. *Nature* 410: 936–939, 2001
25. Takahashi N, Chernavvsky DR, Gomez RA, Igarashi P, Gitelman HJ, Smithies O: Uncompensated polyuria in a mouse model of Bartter's syndrome. *Proc Natl Acad Sci U S A* 97: 5434–5439, 2000
26. Schnermann J, Briggs J: Concentration-dependent sodium chloride transport as the signal in feedback control of glomerular filtration rate. *Kidney Int Suppl* 12: S82–S89, 1982
27. Schweda F, Segerer F, Castrop H, Schnermann J, Kurtz A: Blood pressure-dependent inhibition of renin secretion requires A1 adenosine receptors. *Hypertension* 46: 780–786, 2005
28. Schweda F, Wagner C, Kramer BK, Schnermann J, Kurtz A: Preserved macula densa-dependent renin secretion in A1 adenosine receptor knockout mice. *Am J Physiol Renal Physiol* 284: F770–F777, 2003